Biochemical Pharmacology 81 (2011) 810–818

Contents lists available at ScienceDirect

Biochemical Pharmacology

journal homepage: www.elsevier.com/locate/biochempharm

The food colorant erythrosine is a promiscuous protein–protein interaction inhibitor

Lakshmi Ganesan [a], Emilio Margolles-Clark [b], Yun Song [a], Peter Buchwald [a,b,*]

[a] Department of Molecular and Cellular Pharmacology, Miller School of Medicine, University of Miami, Miami, FL 33136, USA
[b] Diabetes Research Institute, Miller School of Medicine, University of Miami, Miami, FL 33136, USA

ARTICLE INFO

Article history:
Received 12 November 2010
Accepted 27 December 2010
Available online 8 January 2011

Keywords:
Erythrosine
Food color
THP-1 cells
TNF superfamily
Xanthene dyes

ABSTRACT

Following our observation that erythrosine B (FD&C Red No. 3) is a relatively potent inhibitor of the TNF-R–TNFα and CD40–CD154 protein–protein interactions, we investigated whether this inhibitory activity extends to any other protein–protein interactions (PPI) as well as whether any other approved food colors possess such inhibitory activity. We found erythrosine, a poly-iodinated xanthene dye, to be a non-specific promiscuous inhibitor of a number of PPIs within the tumor necrosis factor superfamily (TNF-R–TNFα, CD40–CD154, BAFF-R–BAFF, RANK–RANKL, OX40–OX40L, 4-1BB–4-1BBL) as well as outside of it (EGF-R–EGF) with a remarkably consistent median inhibitory concentration (IC_{50}) in the 2–20 μM (approximately 2–20 mg/L) range. In agreement with this, erythrosine also showed cellular effects including clear cytotoxic effects around this concentration range ($IC_{50} \approx 50$ μM). Among the seven FDA-approved food colorants, only erythrosine showed consistent PPI inhibitory activity in the sub-100 μM range, which might also explain (at least partially) why it also has the lowest approved acceptable daily intake (ADI) (0.1 mg/kg body weight/day). Among a number of xanthene structural analogs of erythrosine tested for activity, rose Bengal, a food colorant approved in Japan, showed similar, maybe even more pronounced, promiscuous inhibitory activity, whereas fluorescein was inactive and gallein, phloxine, and eosin were somewhat active in some of the assays.

1. Introduction

During our recent search for small molecule inhibitors of the CD40–CD154 costimulatory interaction [1–3], which is required for T-cell activation and development of an effective immune response, we found erythrosine B, an FDA-approved food colorant, to be a relatively potent inhibitor (median inhibitory concentration, $IC_{50} \approx 10$ μM) of two protein–protein interactions (PPI) that are members of the tumor necrosis factor (TNF) superfamily, TNF-R–TNFα and CD40–CD154. Since such inhibition could result in unwanted toxic side effects, we investigated whether any other approved food colors possess such inhibitory activity as well as whether this inhibitory activity of erythrosine extends to any other PPIs both within the TNF superfamily and outside of it. Erythrosine B (FD&C Red No. 3, C.I. Acid Red 51, tetraiodofluorescein) (ErB) is a cherry-pink, coal-based food colorant with a poly-iodinated xanthene structure (**1**, Fig. 1) unique among FDA approved food dyes [4]. It is also used as an exclusion dye and a phosphorescent probe for membrane proteins. Similar to other compounds containing a carboxylphenyl group in their structure, ErB can be either in its open-ring acid (**1a**) or in its closed-ring spiro-lactone form (**1b**; Fig. 1) depending on the surrounding solvent conditions. Starting with the 1970s, ErB has been associated with the Feingold hypothesis that food colorants caused hyperkinetic behavior in children [5], a controversial hypothesis with some limited clinical evidence [6,7]. This might be due to some of ErB's effects on the central nervous system (CNS), which include, among others, the inhibition of dopamine uptake [6,8–10]. More recently, ErB has been shown to be a micro-molar inhibitor of a number of important interactions [11–18] (see Section 4). Here, we report the results of our investigation on the *in vitro* inhibitory activity of ErB and compare it to that of other food colorants including all those approved for use in the USA, Europe, and Japan as well as that of some of its structural analogs on important PPIs such TNF-R–TNFα, CD40–CD154, BAFF-R(CD268)–BAFF(CD257), RANK(CD265)–RANKL(CD254), OX40(CD134)–OX40L(CD252), 4-1BB(CD137)–4-1BBL, and EGF-R–EGF.

Abbreviations: ADI, acceptable daily intake; BAFF, B-cell activating factor (CD257); BrdU, bromodeoxyuridine; BSA, bovine serum albumin; DAPI, 4′,6-diamidino-2-phenylindole; EGF, epidermal growth factor; FBS, fetal bovine serum; HRP, horseradish peroxidase; IC_{50}, median inhibitory concentration; K_d, equilibrium dissociation constant of a ligand–receptor complex; PBS, phosphate buffered saline; PPI, protein–protein interaction; RT, room temperature; TNF, tumor necrosis factor.

* Corresponding author at: Diabetes Research Institute, Miller School of Medicine, University of Miami, 1450 NW 10 Ave (R-134), Miami, FL 33136, USA. Tel.: +1 305 243 9657.
E-mail address: pbuchwald@med.miami.edu (P. Buchwald).

0006-2952/$ – see front matter © 2011 Elsevier Inc. All rights reserved.
doi:10.1016/j.bcp.2010.12.020

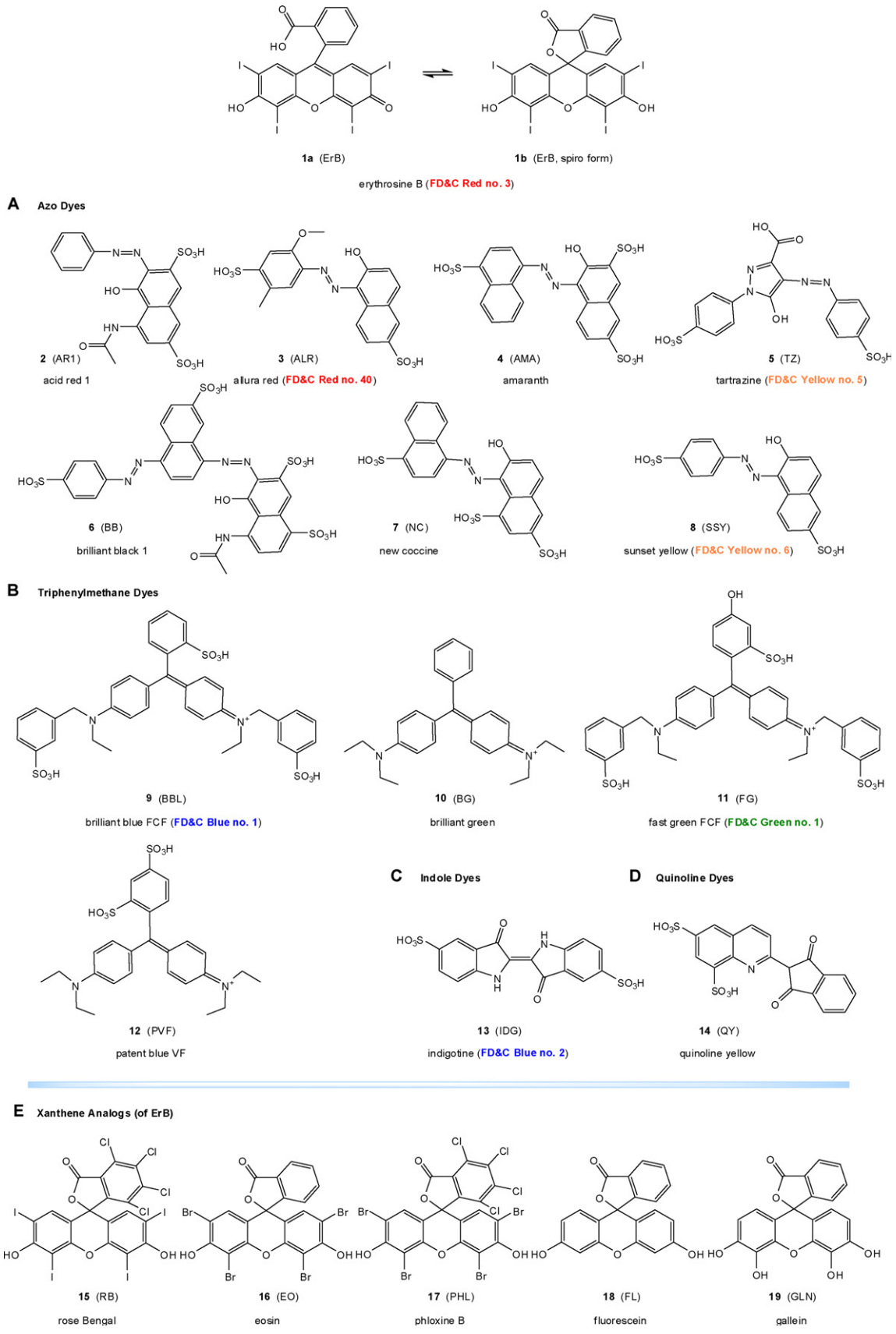

Fig. 1. Chemical structure of the compounds of the present study including food colorants (**1**–**14**) and xanthene analogs of erythrosine (**15**–**19**).

2. Materials and methods

2.1. Materials

All chemicals and reagents used were obtained from Sigma–Aldrich (St. Louis, MO). The monoclonal anti-human CD154 (clone 40804) and anti-human TNF-α antibodies (clone 1825) were purchased from R&D Systems (Minneapolis, MN); the anti-EGFR antibody (clone ICR10) was obtained from Abcam (Cambridge, MA). Purified recombinant Fc-conjugated receptors (CD40, TNF-R1, RANK, BAFF-R, OX40, 4-1BB) and their corresponding FLAG-tagged ligands (CD154, TNFα, RANKL, BAFF, OX40L, 4-1BBL) of the TNF superfamily were obtained from Axxora, LLC (San Diego, CA). The EGF-R was purchased from R&D Systems, and the biotinylated EGF ligand was obtained from Invitrogen (San Diego, CA).

2.2. PPI inhibition assays

ELISA-based screening assays for testing inhibition by compounds of interest were set up as described previously [1,3,19]. Microtiter plates (Nunc F Maxisorp; 96-well) were coated overnight at 4 °C with 100 μL/well of Fc chimeric receptors diluted in PBS 7.2. This was followed by blocking with 200 μL/well of blocking solution (PBS 7.2, 0.05% Tween-20, 1% BSA) for 1 h at RT. The plates were then washed twice using the washing solution (PBS 7.4, 0.05% Tween-20) and dried before the addition of the appropriate FLAG tagged/biotinylated ligands along with different concentrations of test compounds diluted in binding buffer (100 mM HEPES, 0.005% BSA pH 7.2) or protein-containing media (IMDM medium supplemented with 5% FBS) to give a total volume of 100 μL/well. Either anti-FLAG-HRP or streptavidin-HRP conjugate was used to detect the bound FLAG-tagged or biotinylated ligand, respectively. Plates were washed thrice before the addition of 120 μL/well of HRP substrate TMB (3,3′,5,5′-tetramethylbenzidine) and kept in the dark for 30 min. The reaction was stopped using 30 μL 1 M H_2SO_4, and the absorbance was read at 450 nm. The concentrations of receptors used were 0.3 μg/mL for CD40, TNF-R1, and RANK; 0.6 μg/mL for BAFF-R, OX40, and 4-1BB; and 2 μg/mL for EGF-R. The concentrations of the ligands were fixed at 0.02 μg/mL for CD154, TNFα, and RANKL; 0.2 μg/ml for BAFF, OX40L, 4-1BBL; and 0.3 μg/mL for EGF.

2.3. Schild analysis

Schild analysis [20] was done using the same setup described above. The plot was constructed by fixing the concentration of CD40 at 1 μg/mL. The concentration of CD154 was varied from 0 to 10 μg/mL to obtain dose–response curves in the absence or the presence of increasing concentrations (0.08–10 μM) of **1**, direct red 80 (DR80), which has been shown to be a relatively specific CD40–CD154 inhibitor [1], and anti-CD154 antibody (0.13–3.25 nM), which was used as a positive control for competitive behavior. Binding data were fitted with a unified model as described below.

2.4. Cytotoxicity assays

For the BrdU assay, THP-1 human myeloid cells from American Type Culture Collection (Manasses, VA, USA) were cultivated in Roswell Park Memorial Institute (RPMI) media 1640 supplemented with 10% FBS, 100 U/mL penicillin and 100 μg/mL streptomycin, and 50 μM β-mercaptoethanol to a density of 1×10^6 cells per milliliter. The cells were centrifuged and re-suspended in the same medium without FBS and added to a 96-well microtiter plate at a density of 100,000 cells/well in the absence or presence of various concentrations of inhibitors diluted in the same media. The plate was incubated at 37 °C for 24 h. BrdU incorporation was determined using the BrdU cell proliferation kit from Roche (Mannheim, Germany) according to the manufacturer's protocol. For the DAPI assay, THP-1, Jurkat, and HEK293T cells were seeded to a density of 250,000 cells per milliliter in the absence or presence of test compounds for 12 h. Viability upon treatment was determined using a BD LSR II Flow Cytometer (BD Biosciences, San Jose, CA) and the software FlowJo version 7.2.2 (Ashland, OR). The number of live cells was quantified after gating out 4′,6-diamidino-2-phenylindole (DAPI) and cell debris assessed on the basis of forward and side-scatter properties of the untreated samples as reference.

2.5. JNK phosphorylation

THP-1 cells were starved overnight in 25 cm^2 tissue culture flasks in 10 mL/flask at a cell density of 8×10^5 cells/mL in serum-free RPMI supplemented with 100 U/mL penicillin and 100 μg/mL streptomycin, and then stimulated with recombinant human TNFα (Axxora, LLC; 20 ng/mL). Following an initial time-course investigation of the phosphorylation pattern of JNK in THP-1 cells with stimulation times of 5 min, 10 min, 30 min, 1 h, 2 h, 4 h, and 8 h, the 10 min stimulation was selected for the inhibition experiments. In these, TNFα was added immediately after the addition of test compounds (50 μM) or anti-human TNFα monoclonal antibody (2.0 μg/mL, ~13 nM) (R&D Systems). The JNK (c-Jun N-terminal kinase) inhibitor anthra (1, 9-cd)pyrazol-6(2H)-one (SP600125, Sigma–Aldrich) was also used as a positive control (50 μM, 30 min before TNFα ligand induction). At the indicated time points, cells were rapidly washed with ice-cold PBS and lysed with a chilled lysis buffer (10 mM Tris base, 5 mM EDTA, 50 mM NaCl, 1% Triton X-100, 0.5 mM phenylmethylsulfonyl fluoride, 2 mM sodiumorthovanadate, 10 μg/mL leupeptin, 25 μg/mL aprotinin, 1.25 mM NaF, 1 mM sodium pyrophosphate and 10 mM *n*-octyl-β-D-glucopyranoside) for 15 min on ice. Cell debris was removed by centrifugation at 14,000 rpm for 15 min at 4 °C, and the supernatant was immediately transferred to a fresh tube. Solubilized proteins were separated using SDS-PAGE and transferred to a nitrocellulose membrane. P-JNK and JNK (loading control) were visualized with monoclonal antibodies #9251 (Cell Signaling Technology, Beverly, MA) and AF1387 (R&D Systems, Minneapolis, MN), respectively. Protein quantification was performed with NIH Image J software (http://rsb.info.nih.gov/ij/).

2.6. Data fitting and statistics

All binding analyses were done in duplicate or triplicate per plate and repeated at least twice; the averaged data was normalized and used for data fitting and analysis. Binding data were fitted using the standard log inhibitor versus response model:

$$B = 100\frac{[C]}{[C] + \mathrm{IC}_{50}} = 100\frac{1}{1 + 10^{(\log \mathrm{IC}_{50} - \log[C])}} \quad (1)$$

For the Schild analysis, a common Gaddum/Schild EC_{50}-shift model was used to fit all binding data obtained at five different inhibitor concentrations:

$$B = B_{\mathrm{bottom}} + (B_{\mathrm{top}} - B_{\mathrm{bottom}})\frac{[L]^{n_H}}{[L]^{n_H} + \{K_d[1 + ([I]/K_i)^{n_S}]\}^{n_H}} \quad (2)$$

The model was used with unified K_d and K_i values (equilibrium dissociation constants characterizing the CD40–CD154 and the inhibitor bindings, respectively) and unity Hill and Schild slopes ($n_H = 1, n_S = 1$). All fittings were done with GraphPad Prism 5.02 (La Jolla, CA). Cytotoxicity and Western blot data were analyzed by one-way repeated-measures analysis of variance (ANOVA) followed by Tukey's multiple comparison test as a post hoc test for individual differences using GraphPad Prism and a significance level of $p < 0.05$ for all comparisons.

Table 1
Median inhibitory concentrations (IC_{50}) of FDA-approved food colorants for the CD40–CD154, TNF-R1–TNFα, and EGF-R–EGF interactions.

No.	Legend	Compound	USA Food Color	IC_{50} (μM; HEPES)		
				CD40–CD154	TNF-R1–TNFα	EGF-R–EGF
1	ErB	Erythrosine B	FD&C Red no. 3	3	5	3
3	ALR	Allura Red	FD&C Red no. 40	190	>1000	>1000
5	TZ	Tartrazine	FD&C Yellow no. 5	>1000	>1000	>1000
8	SSY	Sunset yellow FCF	FD&C Yellow no. 6	>1000	>1000	>1000
9	BBL	Brilliant Blue FCF	FD&C Blue no. 1	140	>1000	>1000
11	FG	Fast Green FCF	FD&C Green no. 3	70	>1000	>1000
13	IDG	Indigotine	FD&C Blue no. 2	>1000	>1000	>1000

3. Results

3.1. PPI inhibition

A total of fourteen food colors (Fig. 1) approved in the USA, Europe, or Japan [4] – including all seven FDA-approved food colorants – were tested for their activity to inhibit a number of PPIs

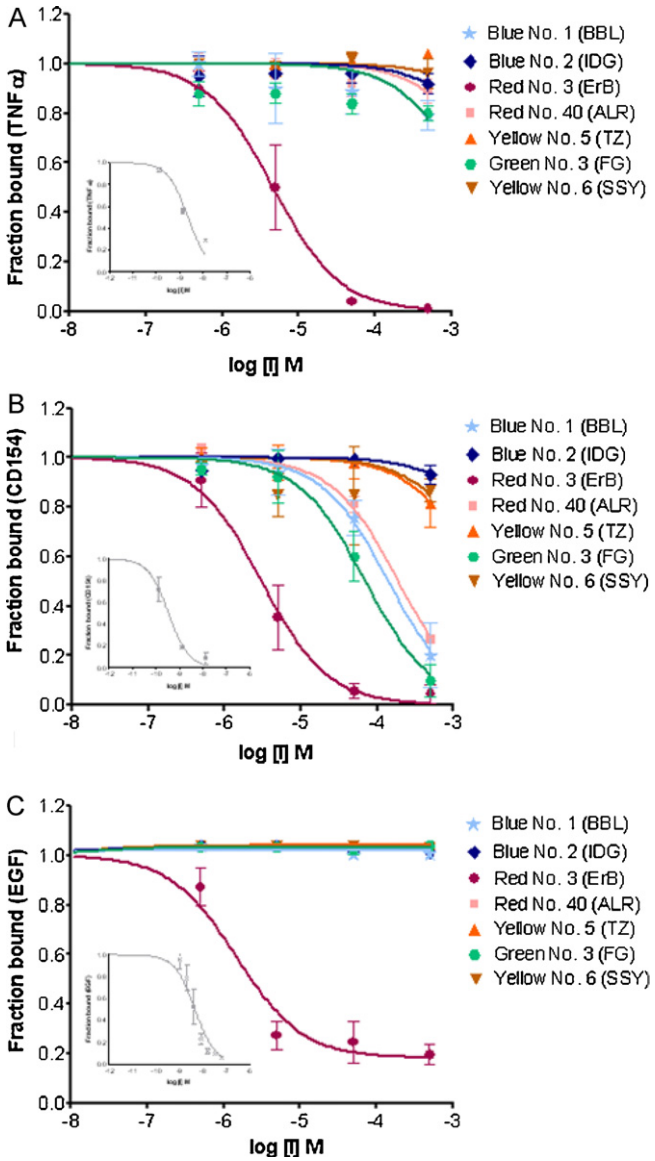

Fig. 2. Concentration-dependent inhibition of human TNF-R1–TNFα (A), CD40–CD154 (B), and EGF-R–EGF (C) interactions by FDA-approved food colorants (see Table 1 for the corresponding IC_{50}s). Smaller insets show inhibition with the corresponding antibodies.

mainly within the TNF superfamily (TNFSF), but also outside of it (Table 1; Fig. 2, Figs. S1 and S2 in Supporting Information). As before [1–3,19], a blocking antibody was included as a positive control in a number of assays (e.g., TNF-R–TNFα, CD40–CD154, BAFF-R–BAFF, and EGF-R–EGF), and in all cases their inhibitory activities with IC_{50}s in the nanomolar (nM) range have been confirmed. Whereas ErB (**1**) consistently showed inhibition in all these assays with a remarkably similar activity, IC_{50}s in the 2–20 μM range (approx. 2–20 mg/L), none of the other food colors **2**–**14** showed significant (i.e., $IC_{50} < 50$ μM) inhibitory activity. Interestingly, **1** seems to maintain considerably inhibitory activity even in the presence of protein containing media, a condition that resulted in about ten-fold loss in activity in these assays for azo-containing organic dyes [1,2], and also a complete loss of activity ($IC_{50} > 500$ μM) for the food colorants **2**–**14** (Table S1).

Since **1** has a unique chemical structure among FDA-approved food colorants, we also tested several close structural analogs including poly-halogenated xanthene analogs such as rose Bengal (**15**), phloxine B (**16**), and eosin (**17**), as well as non-halogenated xanthene analogs such as fluorescein (**18**) and gallein (**19**) to assess the structural basis of the promiscuous inhibitory activity across the spectrum of these PPIs (Table 2). Whereas **1** and **15** showed consistent and promiscuous inhibitory activity, this was considerably diminished in the poly-brominated analogs **16** and **17** and essentially lacking in the non-halogenated fluorescein (**18**). The hydroxyl-substituted gallein (**19**) showed inhibitory activity only in selected interactions (CD40–CD154, RANK–RANKL, and OX40–OX40L) (Table 2; Fig. 3, Fig. S3 in Supporting Information).

3.2. Nature of CD40–CD154 inhibition

In previous studies, we have shown that whereas most other organic dye small molecule inhibitors we identified seem to bind to the surface of CD154 and not CD40, **1** binds with low μM affinity to both [2]. As a preliminary evaluation of the mechanism of inhibition by **1**, i.e., as a first test for the competitive/reversible nature of its inhibitory effect, we performed a Schild analysis [20] as described in Section 2. Dose–response curves were generated by using a fixed concentration of CD40 and varying concentrations of CD154 in the presence of increasing concentrations of inhibitors. As a positive control, an anti-CD154 monoclonal antibody (mAb) was used; its binding data (Fig. 4A) could be fitted well with the unified Gaddum–Schild model (Eq. (2)), and best fit was obtained with a K_d of 1 nM for the CD40–CD154 binding and a pA_2 value of 9.57 (corresponding to K_i of 0.27 nM) for the mAb inhibition – in good agreement with our previous results from straightforward inhibition experiments (e.g., IC_{50} of 0.25 nM ≈ 0.04 μg/mL [1,2,19]). ErB, as well as direct red 80 (DR80), which was included since it has been shown to be a relatively specific inhibitor for CD40–CD154 [1], showed similar profiles (Fig. 4B and C, respectively) indicating competitive/reversible binding with pA_2 values of 6.0 and 5.7 (corresponding to K_is of 1.0 and 1.8 μM), again in good agreement with our previous results from inhibition experiments (IC_{50}s of 2–3 μM for both **1** and DR80, respectively [1–3]).

Table 2
Median inhibitory concentrations (IC_{50}) of **1** and its xanthene analogs (**15**–**19**) for various protein–protein interactions tested here.

No.	Legend	Compound	IC_{50} (μM; HEPES)						
			CD40–CD154	TNF-R1–TNFα	RANK–RANKL	OX40–OX40L	BAFF-R–BAFF	4-1BB–4-1BBL	EGF-R–EGF
1	ErB	Erythrosine B	3	5	2	2	12	11	3
15	RB	Rose Bengal	5	4	2	2	3	3	3
16	PHL	Phloxine B	17	161	8	7	365	20	64
17	EO	Eosin	104	579	47	45	862	261	308
18	FL	Fluorescein	>1000	>1000	>1000	>500	>1000	>1000	>1000
19	GLN	Gallein	6	143	17	4	63	57	398

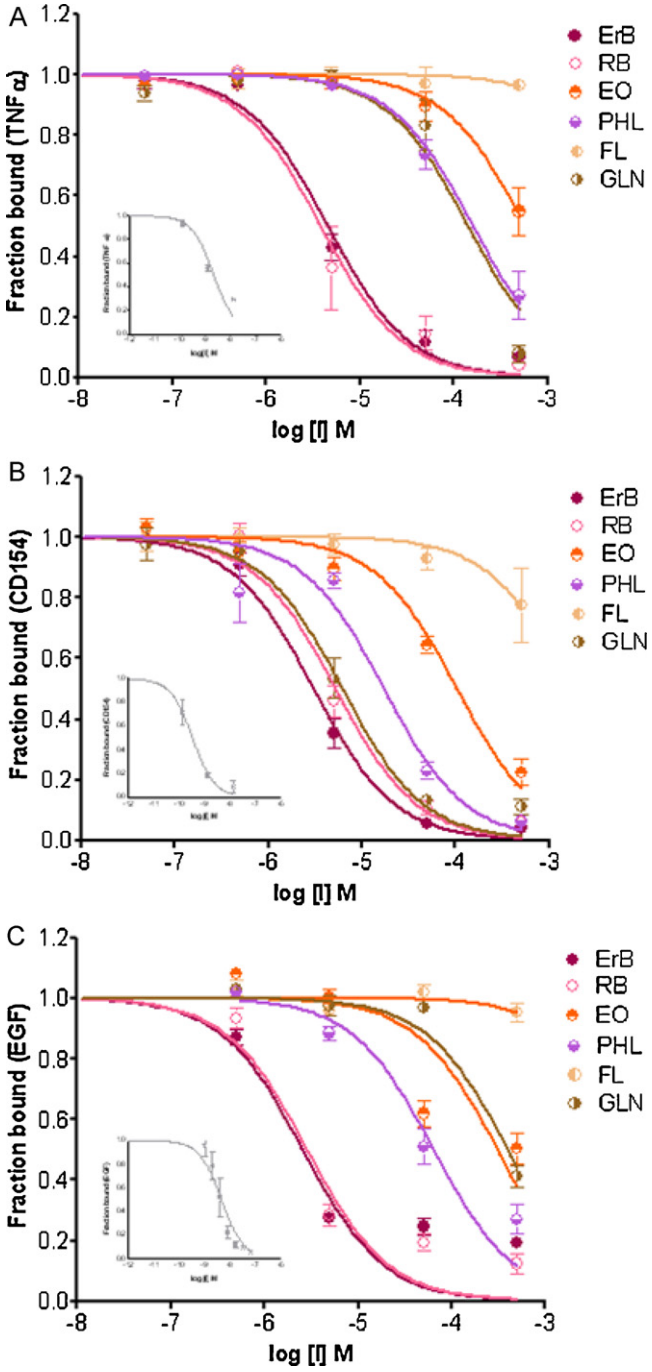

Fig. 3. Concentration-dependent inhibition of human TNFR1–TNFα (A), CD40–CD154 (B), and EGF-R–EGF (C) interactions by structural analogs of erythrosine (ErB, 1) (Table 2).

3.3. Cytotoxicity and cell effects

To test whether this promiscuous *in vitro* protein inhibitory activity translates into toxic effects, we determined the cytotoxic potential of **1** in three different cells: THP-1 (human monocytic leukemia cells), Jurkat (immortalized T lymphocyte cells), and HEK293T (human embryonic kidney derived cells) compared to other control organic dyes. Toxic effects were assessed both by an apoptosis assay (DAPI staining analyzed by flow cytometry) and a

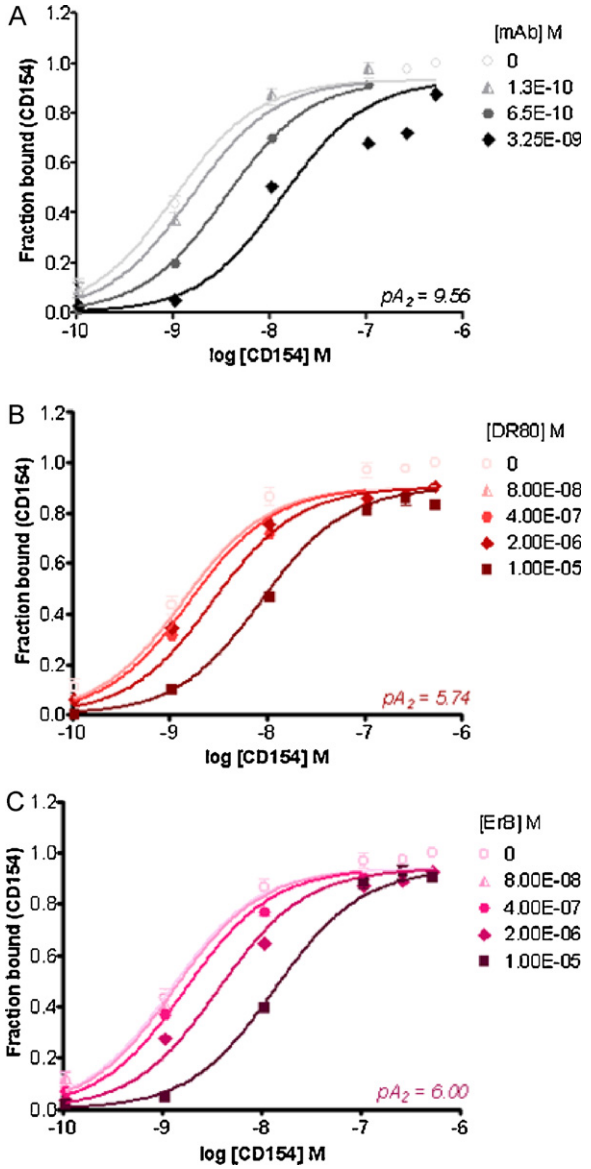

Fig. 4. Schild analysis of the CD40–CD154 inhibitory activity for an inhibitory antibody (mAb; A), direct red 80 (DR80; B), and **1** (ErB; C).

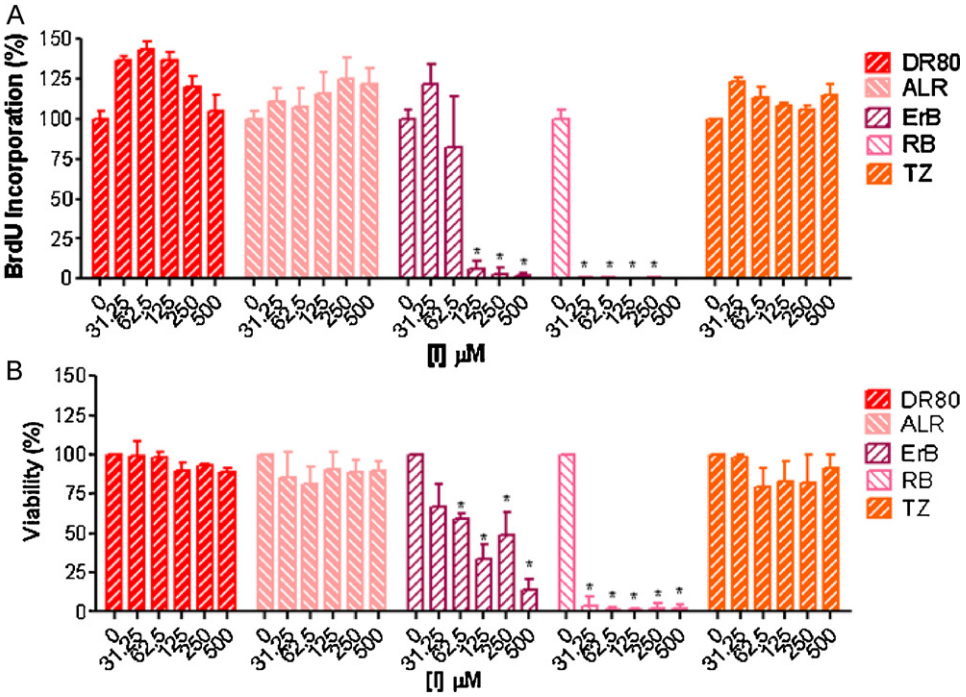

Fig. 5. Cell toxicities of **1** (ErB), **3** (ALR), **5** (TZ), **15** (RB), and DR80 as assessed by a standard proliferation assay (BrdU; A) and an apoptosis assay (DAPI exclusion; B) in THP-1 cells. Data (average ± SD for $n = 3$ independent experiments with triplicates for each condition) were analyzed by ANOVA with Tukey's post hoc test and asterisk (*) indicates statistically significant differences ($p < 0.001$) versus untreated controls (0).

cell proliferation assay (BrdU incorporation) (Fig. 5 and Fig. S4 Supporting Information). Whereas both promiscuous inhibitors **1** and **15** clearly showed signs of cytotoxicity with IC_{50}s of less than 100 μM for **1** and even less for **15**, the corresponding comparators used, including DR80, which has a similar K_i for the CD40–CD154 inhibition [1], and **3** (allura red), which is the other FDA-approved red food colorant, showed no toxic effect up to 500 μM concentrations (Fig. 5) – a clear indication of the possible detrimental effects related to the nonspecific inhibitory activity of **1** and **15**.

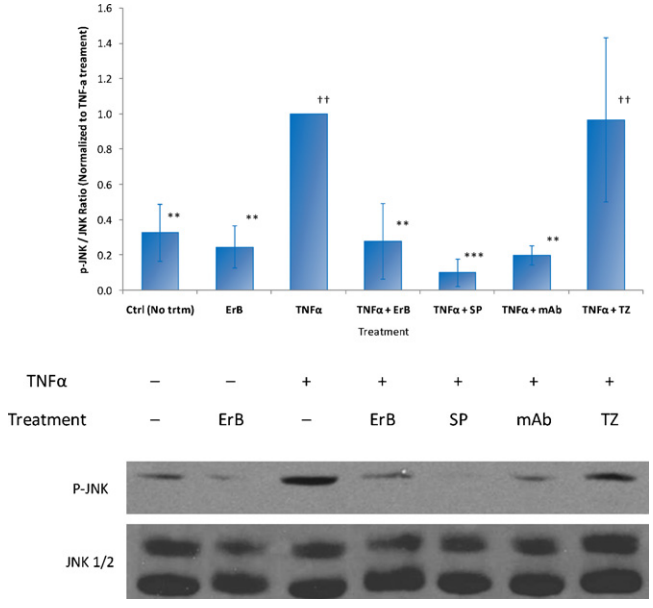

Fig. 6. Inhibition of TNFα-induced JNK phosphorylation by **1** in THP cells as evidenced by Western blot analysis. Data (fraction of JNK phosphorylated, normalized with TNFα treatment as reference; average ± SD for $n = 3$ independent experiments) were analyzed by ANOVA with Tukey's post hoc test, and †† and ** indicate statistically significant differences ($p < 0.01$) versus untreated control and TNFα-treatment, respectively.

Finally, as a further confirmation that the inhibitory activity of **1** translates into cellular effects, we also evaluated its effect on TNFα–induced JNK (c-Jun N-terminal kinase) phosphorylation in THP-1 cells by Western blotting. JNK is a member of the mitogen-activated protein kinase (MAPK) family, and it is a stress-response kinase activated by proinflammatory cytokines and growth factors coupled to membrane receptors or by various stimuli, such as heat shock, UV irradiation, protein synthesis inhibitors, and elevated levels of reactive oxygen intermediates (ROI), through nonreceptor pathways. TNFα (20 ng/mL) clearly caused activation of this pathway significantly increasing the phosphorylated fraction of JNK (predominantly that of one isoform [21,22]) even after a short incubation (5 min), and this was reversed by the anti-TNFα antibody (2.0 μg/mL) as well as by **1** (50 μM) and the known JNK inhibitor SP600125, but not **5** (TZ), which was used as a negative control (Fig. 6). We selected this assay because it can be performed with short incubation times avoiding possible confounding effects due to cytotoxicity following longer incubations at these concentrations.

4. Discussion

Following our initial observation that **1**, an FDA-approved food colorant (FD&C Red No. 3, erythrosine), is a relatively potent and non-specific inhibitor of a number of important receptor–ligand-type PPIs within the TNFSF [1], here, we investigated whether any other approved food colors possess such inhibitory activity. Among FDA approved food colorants (**1**, **3**, 5, **8**, **9**, **11**, and **13**) [4], this inhibitory activity seems to be unique for **1**. Here, we found compound **1** to inhibit a large variety of PPIs within the TNF receptor–ligand superfamily (TNFRSF–TNFSF) as well as outside of it (EGF-R–EGF) with a remarkably consistent IC_{50} in the 2–20 μM range (approximately 2–20 mg/L) (Table 1, Fig. 2, Figs. S1 and S2). Furthermore, beside its long-known inhibitory activity on dopamine uptake ($IC_{50} \approx 50$ μM) [6,8–10] or acetylcholine release [23],

Table 3
Confirmed inhibitory activities of erythrosine (**1**).

Protein/enzyme	IC_{50} (μM)	Reference
TNF superfamily (Table 2)	2–15	Present work
EGF-R–EGF	3	Present work
Catecholamine (dopamine) uptake	≈50	[6,8–10]
Acetylcholine release	≈10	[23]
ATPases	10–30	[51,60]
Insulin–insulin receptor	11	[12]
Protein tyrosine phoshatases (PTP1B, TC-PTP, YPTP1)	5–25	[15]
UDP glucuronosyltransferase (UGT1A6)	50	[13,14]
Cytochrome P450 (CYP3A4)	8	[13,14]
Aromatase (CYP19)	≈0.3	[61]
P-glycoprotein (P-gp)	16	[13,14]
Galactokinase	≈10	[16]
Sulfotransferase	5–10	[18]
ADP transport via the ADP/ATP carrier	≈1	[25]
ATP-dependent glutamate uptake	35	[17]
DNA–anti-DNA antibody (IgG2b) interaction	≈10	[24]

1 has also been shown more recently to inhibit various other protein interactions or activities within the same concentration range (Table 3) [12–18,24,25]. It also showed some evidence of reducing motor activity by reducing serotonergic activity in rodents [26]. In rat spleen lymphocytes, **1** as well as **15** stimulated the production of immunoglobulin IgE while inhibiting the production of IgG and IgM at 50 μM [27].

Since among FDA-approved food colorants, **1** has a unique poly-iodinated xanthene structure, we also tested some of its structural analogs (**15**–**19**, Fig. 1). Among them, rose Bengal (**15**), a poly-chlorinated analog of **1** and a food colorant approved in Japan, showed similar, maybe even more pronounced promiscuous inhibitory activity. The non-specific inhibitory activity was somewhat diminished in the poly-brominated analogs (**16** and **17**) and essentially lacking in the non-iodinated fluorescein (**18**) (Fig. 3). The non-iodinated, but hydroxyl-substituted gallein (**19**) showed inhibitory activity in a few selected interactions. Gallein, and its close structural analog M119 (NSC119910), but not fluorescein have also been shown to inhibit the interaction of the G-protein subunit Gβγ with effectors such as phosphoinositide 3-kinase γ (PI3-kinase γ) [28]. The exact mechanism of this promiscuous inhibitory activity is somewhat unclear at this point; the poly-iodinated **1** and **15** bound with low micromolar affinity to all proteins we tested so far. Since inhibition of protein–protein interactions with small molecules is a challenging task [29,30], the existence of such low-micromolar promiscuous inhibitors is intriguing. The Schild analyses (Fig. 4 and its reversed version with plate-coated CD154 – data not shown) seem to indicate at least a partially reversible (surmountable) mechanism as inhibition by **1** could be overcome with increasing CD40 or CD154 concentrations.

Biochemical screening assays are often confounded by the presence of compounds that are known 'promiscuous inhibitors' [11], 'frequent hitters' [31], or contain chemically reactive functional groups such as protein-reactive electrophilic false positives as well as chelator and polyionic 'warheads' [32]. Compound **1**, together with several other dye compounds, have been found to act as promiscuous inhibitors in high-throughput screening (HTS) assays, and polymolecular conglomeration [33,34]/aggregation [11,35] have been suggested as possible mechanisms. To investigate the possibility of aggregation effects, we repeated the CD40–CD154 binding assays in the presence of a non-ionic detergent (Triton X-100, 0.05% and 0.5%) as recommended for the detection of promiscuous inhibitors [36], but observed no significant effect on IC_{50}s for **1** (data not shown). Xanthene dyes can aggregate in aqueous solutions, but at higher concentrations; for example, with K_ds around 1 mM for dimerization of **1** and its structural analogs [37]. Loss of activity upon dilution is yet another characteristic of inhibition by aggregates, and this was not observed with **1** whose activity persisted for a long time even after dilution.

A mechanism with reversible binding and multiple possible binding sites on the protein surface, at least some of which overlap with the binding site of the protein partner, as it has been suggested on the basis of spectroscopic experimental evidence in the case of insulin – insulin receptor inhibition by **1** [38] and in the case of **1** binding to BSA [39], seems more likely here as well. Compound **1**, as well as **15**, especially in their spiro isomeric forms, are not only relatively large, very flat structures, but also particularly rigid ones having no rotatable bonds that can relatively easily bind to flat, hydrophobic pockets. Entropy and more specifically loss of entropy due to binding plays a critical role in modulating binding efficiency, but predicting its contribution is non-trivial and controversial [40–42]. The barrier to binding due to the loss of rigid-body entropy varies across a considerable range [43], its value being somewhere around 15–20 kJ/mol, which corresponds to about three orders of magnitude in affinity, according to a more recent estimate [40]. This might explain at least part of the promiscuous binding activity of **1** and **15**: a relatively large, flat molecular size with a rigid structure capable of van der Waals interactions (including aromatic stacking) with no entropy loss due to blocking of rotational freedoms. Presence of the large iodine substituents also seems important for the non-specific inhibitory activity; the smaller the size the less prominent the promiscuous inhibitory activity found in the assays performed here.

Xanthene dyes such as **1** and **15** are well-known sensitizers enhancing the photosensitized oxidation of proteins that might bind non-covalently and enhance photosensitized oxidation of biomolecules [39,44,45]. We repeated the CD40–CD154 PPI inhibitory assay with dark and light conditions in parallel and found the activity of **1** and **15** to diminish in dark about 5–10-fold whereas those of DR80 and anti-CD154 mAb were virtually unchanged (Fig. S5, Supporting Information). Hence, photosensitization might account for some of the inhibiting activity seen under *in vitro* conditions, where light is a factor, but most of the activity is still retained in dark. Light showed about a similar enhancing effect on the inhibitory effect of **1** on the binding of ouabain to the digitalis receptor [46]. For comparison, for a set of compounds identified as possible PPI inhibitors for TNF-R–TNFα that ultimately turned out to modify the receptor covalently by a photochemical reaction due to exposure to light, the activity was 50-fold to >1000-fold diminished in dark [47]. The presence of bromine or iodine atoms enhances the yield of intersystem crossing to the reactive triplet state of these dyes, and tetraiodo xanthene derivatives, such as **1** and **15**, show the greatest photosensitizing activity [48]. Because of their photosensitized oxidative ability, xanthene dyes, and in particular **1**, **15**, and **16**, have also been explored as possible light-activated insecticides [48] or antimicrobials [49]. Intralesionally applied **15** is being investigated as a possible chemoablation agent in metastatic melanoma [50].

There also have been suggestions that some of these xanthenes dyes, and in particular **1**, might be capable of specific interactions with the nucleotide binding sites of membrane energy-transducing enzymes (such as ATPases) because of the structural overlap between ErB and AMP (adenosine monophosphate) [51] or ADP [25], and such binding sites are present on many different proteins [52]. However, CPK structures clearly reveal that even if stick structures might allow some overlap, true structural analogy is lacking due to the large size of the iodine substituents (Fig. S6), and molecular size is, of course, a major determinant of binding

ability [53,54]. In fact, better overlap might be possible with the flavine part of FAD (flavine adenine dinucleotide).

Toxicity is an obvious concern related to the promiscuous inhibitory activity, especially that possible toxic side effects are a particularly controversial issue for synthetic food colorants. These compounds are relatively nontoxic, but this is certainly a contentious subject. Various adverse reactions, mainly possible behavioral alterations and food allergies, have been often – and controversially – linked to food colorants [55]. Erythrosine (**1**) itself has been associated with the controversial Feingold hypothesis that food colorants caused hyperkinetic behavior in children [5–7]. For the iodine-containing **1**, thyroid toxicity was also a major concern [56]. One relatively recent study even found a number of food colors, including **1**, **3**, and **5** as well as **15** and **16** to be genotoxic causing dose-related DNA damage in the gastrointestinal organs at doses (10 or 100 mg/kg) that are not very far from the acceptable daily intakes (ADIs) (Table 1) [57]. It is important to note that the current ADI for **1** is 0.1 mg/kg body weight/day, already considerably lower than that of any other FDA-approved food color, e.g., 7 mg/kg body weight/day for allura red (**3**) or 7.5 for tartrazine (**5**) (Table S1) [4]. For **1**, this value is based on the no observed effect level (NOEL) of 1 mg/kg body weight/day (60 mg per person per day) for effects on thyroid function in humans observed at the next highest dose of 3.3 mg/kg body weight/day and obtained using a 10-fold safety factor [58]. Considering the relatively potent promiscuous inhibitory activity of **1**, which is unique among food colorants, such a low ADI seems to be well-justified. On the other hand, since the nonspecific inhibitory activity of **1** (as well as **15**) seems to become a concern at concentrations starting around a 2–20 μM (approx. 2–20 mg/L) range, related effects should not be an issue if the ADI guidelines (0.1 mg/kg body weight/day) are followed. Nevertheless, because **1** is a quite hydrophobic (log $P_{o/w} > 5$) and blood-brain barrier (BBB)-permeable molecule, considerable tissue accumulation might take place (e.g., biological toxicity seemed log *P*-related in xanthenes dyes [59]); hence, adherence to the ADI guidelines would seem a reasonable precaution, and it should be extended to rose Bengal (**15**) as well where it is approved for food use.

Acknowledgement

Financial support by the Diabetes Research Institute Foundation (www.diabetesresearch.org) is gratefully acknowledged.

Appendix A. Supplementary data

Supplementary data associated with this article can be found, in the online version, at doi:10.1016/j.bcp.2010.12.020.

References

[1] Margolles-Clark E, Umland O, Kenyon NS, Ricordi C, Buchwald P. Small molecule costimulatory blockade: organic dye inhibitors of the CD40–CD154 interaction. J Mol Med 2009;87:1133–43.
[2] Buchwald P, Margolles-Clark E, Kenyon NS, Ricordi C. Organic dyes as small molecule protein–protein interaction inhibitors for the CD40-CD154 costimulatory interaction. J Mol Recogn 2010;23:65–73.
[3] Margolles-Clark E, Kenyon NS, Ricordi C, Buchwald P. Effective and specific inhibition of the CD40–CD154 costimulatory interaction by a naphthalenesulphonic acid derivative. Chem Biol Drug Des 2010;76:305–13.
[4] Glória MBA. Synthetic Colorants. In: Hui YH, editor. Handbook of food science, technology, and engineering. Boca Raton: CRC Press; 2006. p. 86–115.
[5] Feingold BF. Hyperkinesis and learning disabilities linked to artificial food flavors and colors. Am J Nurs 1975;75:797–803.
[6] Silbergeld EK, Anderson SM. Artificial food colors and childhood behavior disorders. Bull N Y Acad Med 1982;58:275–95.
[7] Schab DW, Trinh NH. Do artificial food colors promote hyperactivity in children with hyperactive syndromes? A meta-analysis of double-blind placebo-controlled trials. J Dev Behav Pediatr 2004;25:423–34.
[8] Lafferman JA, Silbergeld EK. Erythrosin B inhibits dopamine transport in rat caudate synaptosomes. Science 1979;205:410–2.
[9] Logan WJ, Swanson JM. Erythrosin B inhibition of neurotransmitter accumulation by rat brain homogenate. Science 1979;206:363–4.
[10] Mailman RB, Ferris RM, Tang FL, Vogel RA, Kilts CD, Lipton MA, et al. Erythrosine (Red No. 3) and its nonspecific biochemical actions: what relation to behavioral changes? Science 1980;207:535–7.
[11] McGovern SL, Caselli E, Grigorieff N, Shoichet BK. A common mechanism underlying promiscuous inhibitors from virtual and high-throughput screening. J Med Chem 2002;45:1712–22.
[12] Schlein M, Ludvigsen S, Olsen HB, Andersen AS, Danielsen GM, Kaarsholm NC. Properties of small molecules affecting insulin receptor function. Biochemistry 2001;40:13520–8.
[13] Furumiya K, Mizutani T. Inhibition of human CYP3A4, UGT1A6, and P-glycoprotein with halogenated xanthene food dyes and prevention by superoxide dismutase. J Toxicol Environ Health A 2008;71:1307–13.
[14] Mizutani T. Toxicity of xanthene food dyes by inhibition of human drug-metabolizing enzymes in a noncompetitive manner. J Environ Publ Health 2009;953952. doi: 10.1155/2009/953952.
[15] Shrestha S, Bhattarai BR, Lee K-H, Cho H. Some of the food color additives are potent inhibitors of human protein tyrosine phosphatases. Bull Korean Chem Soc 2006;27:1567–71.
[16] Wierenga KJ, Lai K, Buchwald P, Tang M. High-throughput screening for human galactokinase inhibitors. J Biomol Screen 2008;13:415–23.
[17] Bole DG, Ueda T. Inhibition of vesicular glutamate uptake by Rose Bengal-related compounds: structure–activity relationship. Neurochem Res 2005;30:363–9.
[18] Bamforth KJ, Jones AL, Roberts RC, Coughtrie MW. Common food additives are potent inhibitors of human liver 17 alpha-ethinyloestradiol and dopamine sulphotransferases. Biochem Pharmacol 1993;46:1713–20.
[19] Margolles-Clark E, Jacques-Silva MC, Ganesan L, Umland O, Kenyon NS, Ricordi C, et al. Suramin inhibits the CD40–CD154 costimulatory interaction: a possible mechanism for immunosuppressive effects. Biochem Pharmacol 2009;77:1236–45.
[20] Kenakin TP. A pharmacology primer. Theory, applications, and methods. Burlington, MA: Academic Press; 2006.
[21] Dreskin SC, Thomas GW, Dale SN, Heasley LE. Isoforms of Jun kinase are differentially expressed and activated in human monocyte/macrophage (THP-1) cells. J Immunol 2001;166:5646–53.
[22] Ferlito M, Romanenko OG, Ashton S, Squadrito F, Halushka PV, Cook JA. Effect of cross-tolerance between endotoxin and TNF-α or IL-1β on cellular signaling and mediator production. J Leukocyte Biol 2001;70:821–9.
[23] Augustine Jr GJ, Levitan H. Neurotransmitter release from a vertebrate neuromuscular synapse affected by a food dye. Science 1980;207:1489–90.
[24] Ben-Chetrit E, Eilat D, Ben-Sasson SA. Specific inhibition of the DNA-anti-DNA immune reaction by low molecular weight anionic compounds. Immunology 1988;65:479–85.
[25] Majima E, Yamaguchi N, Chuman H, Shinohara Y, Ishida M, Goto S, et al. Binding of the fluorescein derivative eosin Y to the mitochondrial ADP/ATP carrier: characterization of the adenine nucleotide binding site. Biochemistry 1998;37:424–32.
[26] Dalal A, Poddar MK. Short-term erythrosine B-induced inhibition of the brain regional serotonergic activity suppresses motor activity (exploratory behavior) of young adult mammals. Pharmacol Biochem Behav 2009;92:574–82.
[27] Kuramoto Y, Yamada K, Lim BO, Sugano M. Stimulating effect of xanthene dyes on immunoglobulin produced in vitro by rat spleen lymphocytes. Biosci Biotechnol Biochem 1997;61:723–5.
[28] Lehmann DM, Seneviratne AM, Smrcka AV. Small molecule disruption of G protein beta gamma subunit signaling inhibits neutrophil chemotaxis and inflammation. Mol Pharmacol 2008;73:410–8.
[29] Wilson AJ. Inhibition of protein–protein interactions using designed molecules. Chem Soc Rev 2009;38:3289–300.
[30] Buchwald P. Small-molecule protein–protein interaction inhibitors: therapeutic potential in light of molecular size, chemical space, and ligand binding efficiency considerations. IUBMB Life 2010;62:724–31.
[31] Roche O, Schneider P, Zuegge J, Guba W, Kansy M, Alanine A, et al. Development of a virtual screening method for identification of "frequent hitters" in compound libraries. J Med Chem 2002;45:137–42.
[32] Rishton GM. Nonleadlikeness and leadlikeness in biochemical screening. Drug Discov Today 2003;8:86–96.
[33] Roterman I, No KT, Piekarska B, Kaszuba J, Pawlicki R, Rybarska J, et al. Bisazo dyes—studies on the mechanism of complex formation with IgG modulated by heating or antigen binding. J Physiol Pharmacol 1993;44:213–32.
[34] Stopa B, Gorny M, Konieczny L, Piekarska B, Rybarska J, Skowronek M, et al. Supramolecular ligands: monomer structure and protein ligation capability. Biochimie 1998;80:963–8.
[35] Shoichet BK. Screening in a spirit haunted world. Drug Discov Today 2006;11:607–15.
[36] Feng BY, Shoichet BK. A detergent-based assay for the detection of promiscuous inhibitors. Nat Protoc 2006;1:550–3.
[37] Valdes-Aguilera O, Neckers DC. Aggregation phenomena in xanthene dyes. Acc Chem Res 1989;22:171–7.

[38] Schlein M, Ludvigsen S, Olsen HB, Dunn MF, Kaarsholm NC. Spectroscopic characterization of insulin and small molecule ligand binding to the insulin receptor. Spectroscopy 2002;16:147–59.
[39] Zhang Y, Görner H. Photoprocesses of xanthene dyes bound to lysozyme or serum albumin. Photochem Photobiol 2009;85:677–85.
[40] Murray CW, Verdonk ML. The consequences of translational and rotational entropy lost by small molecules on binding to proteins. J Comput Aided Mol Des 2002;16:741–53.
[41] Reynolds CH, Tounge BA, Bembenek SD. Ligand binding efficiency: trends, physical basis, and implications. J Med Chem 2008;51:2432–8.
[42] Tirado-Rives J, Jorgensen WL. Contribution of conformer focusing to the uncertainty in predicting free energies for protein–ligand binding. J Med Chem 2006;49:5880–4.
[43] Reynolds CH, Bembenek SD, Tounge BA. The role of molecular size in ligand efficiency. Bioorg Med Chem Lett 2007;17:4258–61.
[44] Mignaco JA, Barrabin H, Scofano HM. ATPase and phosphatase activities are differentially inhibited by photo-oxidation of the sarcoplasmic reticulum Ca(2+)-ATPase. Biochim Biophys Acta 1997;1321:252–8.
[45] Davies MJ. Singlet oxygen-mediated damage to proteins and its consequences. Biochem Biophys Res Commun 2003;305:761–70.
[46] Hnatowich M, LaBella FS. Light-enhanced inhibition of ouabain binding to digitalis receptor in rat brain and guinea pig heart by the food dye erythrosine. Mol Pharmacol 1982;22:687–92.
[47] Carter PH, Scherle PA, Muckelbauer JK, Voss ME, Liu RQ, Thompson LA, et al. Photochemically enhanced binding of small molecules to the tumor necrosis factor receptor-1 inhibits the binding of TNF-alpha. Proc Natl Acad Sci USA 2001;98:11879–84.
[48] Ben Amor T, Jori G. Sunlight-activated insecticides: historical background and mechanisms of phototoxic activity. Insect Biochem Mol Biol 2000;30: 915–25.
[49] Waite JG, Yousef AE. Chapter 3: antimicrobial properties of hydroxyxanthenes. Adv Appl Microbiol 2009;69:79–98.
[50] Thompson JF, Hersey P, Wachter E. Chemoablation of metastatic melanoma using intralesional Rose Bengal. Melanoma Res 2008;18:405–11.
[51] Neslund GG, Miara JE, Kang JJ, Dahms AS. Specific interactions of xanthene dyes with nucleotide-binding sites of membrane energy-transducing enzymes and carriers. Curr Top Cell Regul 1984;24:447–69.
[52] Saito M, Go M, Shirai T. An empirical approach for detecting nucleotide-binding sites on proteins. Protein Eng Des Sel 2006;19:67–75.
[53] Buchwald P. General linearized biexponential model for QSAR data showing bilinear-type distribution. J Pharm Sci 2005;94:2355–79.
[54] Buchwald P. Glucocorticoid receptor binding: a biphasic dependence on molecular size as revealed by the bilinear LinBiExp model. Steroids 2008; 73:193–208.
[55] MacGibbon B. Adverse reactions to food additives. Proc Nutr Soc 1983;42:233–40.
[56] Poulsen E. Case study: erythrosine. Food Addit Contam 1993;10:315–23.
[57] Sasaki YF, Kawaguchi S, Kamaya A, Ohshita M, Kabasawa K, Iwama K, et al. The comet assay with 8 mouse organs: results with 39 currently used food additives. Mutat Res 2002;519:103–19.
[58] Joint FAO/WHO Expert Committee on Food Additives. Evaluation of certain food additives and contaminants, 37th Report. WHO Technical Report Series, 806. Geneva: World Health Organization, 1991.
[59] Levitan H. Food, drug, and cosmetic dyes: biological effects related to lipid solubility. Proc Natl Acad Sci USA 1977;74:2914–8.
[60] Swann AC. Brain (Na^+, K^+)-ATPase: biphasic interaction with erythrosin B. Biochem Pharmacol 1982;31:2185–90.
[61] Satoh K, Nonaka R, Ishikawa F, Ogata A, Nagai F. In vitro screening assay for detecting aromatase activity using rat ovarian microsomes and estrone ELISA. Biol Pharm Bull 2008;31:357–62.